Title

Cyanobacterial production of plant essential oils

Journal

Planta, 248(4)

ISSN

0032-0935

Authors

Formighieri, Cinzia

Melis, Anastasios

Publication Date

2018-10-01

DOI

10.1007/s00425-018-2948-0

Peer reviewed

Planta (2018) 248:933–946
https://doi.org/10.1007/s00425-018-2948-0

ORIGINAL ARTICLE

Cyanobacterial production of plant essential oils

Cinzia Formighieri[1] · **Anastasios Melis**[1]

Received: 20 April 2018 / Accepted: 25 June 2018 / Published online: 4 July 2018

Abstract

Main conclusion ***Synechocystis*** **(a cyanobacterium) was employed as an alternative host for the production of plant essential oil constituents. β-Phellandrene synthase (*PHLS*) genes from different plants, when expressed in *Synechocystis*, enabled synthesis of variable monoterpene hydrocarbon blends, converting *Synechocystis* into a cell factory that photosynthesized and released useful products.**

Monoterpene synthases are secondary metabolism enzymes that catalyze the generation of essential oil constituents in terrestrial plants. Essential oils, including monoterpene hydrocarbons, are of interest for their commercial application and value. Therefore, heterologous expression of monoterpene synthases for high-capacity essential oil production in photosynthetic microorganism transformants is of current interest. In the present work, the cyanobacterium *Synechocystsis* PCC 6803 was employed as an alternative host for the production of plant essential oil constituents. As a case study, β-phellandrene synthase (*PHLS*) genes from different plants were heterologously expressed in *Synechocystis*. Genomic integration of individual *PHLS*-encoding sequences endowed *Synechocystis* with constitutive monoterpene hydrocarbons generation, occurring concomitant with photosynthesis and cell growth. Specifically, the β-phellandrene synthase from *Lavandula angustifolia* (lavender), *Solanum lycopersicum* (tomato), *Pinus banksiana* (pine), *Picea sitchensis* (Sitka spruce) and *Abies grandis* (grand fir) were active in *Synechocystis* transformants but, instead of a single product, they generated a blend of terpene hydrocarbons comprising β-phellandrene, α-phellandrene, β-myrcene, β-pinene, and δ-carene with variable percentage ratios ranging from < 10 to > 90% in different product combinations and proportions. Our results suggested that PHLS enzyme conformation and function depends on the cytosolic environment in which they reside, with the biochemical properties of the latter causing catalytic deviations from the products naturally observed in the corresponding gene-encoding plants, giving rise to the terpene hydrocarbon blends described in this work. These findings may have commercial application in the generation of designer essential oil blends and will further assist the development of heterologous cyanobacterial platforms for the generation of desired monoterpene hydrocarbon products.

Keywords Cyanobacteria · Essential oils · Fusion protein · Metabolic engineering · Monoterpenes · Phycocyanin

Abbreviations

cmR	Chloramphenicol resistance cassette from *Escherichia coli*
cpcB	The phycocyanin β-subunit encoding gene
Dcw	Dry cell weight
GPPS	geranyl-diphosphate (GPP) synthase
SlNPPS	neryl-diphosphate (NPP) synthase from *Solanum lycopersicum*
AgPHLS	β-phellandrene synthase from *Abies grandis*

Cinzia Formighieri and Anastasios Melis authors have read and approved the manuscript.

Electronic supplementary material The online version of this article (https://doi.org/10.1007/s00425-018-2948-0) contains supplementary material, which is available to authorized users.

✉ Anastasios Melis
melis@berkeley.edu

[1] Plant and Microbial Biology, University of California, Berkeley, CA 94720-3102, USA

LaPHLS	β-phellandrene synthase from *Lavandula angustifolia*
SlPHLS	β-phellandrene synthase from *Solanum lycopersicum*
PbPHLS	β-phellandrene synthase from *Pinus banksiana*
PsPHLS	β-phellandrene synthase from *Picea sitchensis*
Synechocystis	*Synechocystis* sp. PCC 6803

Introduction

Cyanobacteria are suitable hosts for heterologous production of plant essential oils that have commercial value in the synthetic chemistry, pharmaceutical and cosmetics industries, and in household cleaning applications. Essential oils, such as monoterpene hydrocarbons, are naturally produced as secondary metabolites by several terrestrial plant species (Lane et al. 2010). Development of heterologous microbial systems for essential oils production is a valuable alternative to meet increasing product demand as compared to extraction from the plant biomass. Earlier work from this lab applied heterologous expression in cyanobacteria of the β-phellandrene synthase (*PHLS*) gene from *Lavandula angustifolia* (lavender). This single-gene transformation was necessary and sufficient to endow *Synechocystis* sp. PCC 6803 (*Synechocystis*) with the biosynthesis of β-phellandrene (a monoterpene hydrocarbon), emanating from the photosynthesis-associated cellular metabolism (Bentley et al. 2013; Formighieri and Melis 2014a, 2015).

Leaves of *L. angustifolia* contain essential oils, primarily β-phellandrene in the range of 0.7–2.9 mg g^{-1} fresh weight (Demissie et al. 2011). The *LaPHLS* encoding sequence was identified by microarray analysis to be highly transcribed in young lavender leaves. By in vitro assay, the LaPHLS enzyme was shown to use geranyl-diphosphate (GPP) as substrate and to produce β-phellandrene as the major product (> 86%), followed by limonene, consistent with the promiscuous activity of monoterpene synthases to convert reactants into multiple terpene hydrocarbon products (Demissie et al. 2011). In contrast to higher plants, cyanobacteria and other aquatic microorganisms typically do not have the ability to generate monoterpene hydrocarbons, or other plant essential oils, as they lack the terpene synthase genes required for their synthesis (Van Wagoner et al. 2007). Constitutive generation of β-phellandrene in *Synechocystis* was achieved only upon heterologous expression of the *LaPHLS* encoding sequence. In particular, earlier work identified the slow k_{cat} of the enzyme to be the main factor limiting rate and yield of product generation, a limitation that was overcome by increasing the concentration of the terpene synthase in the cyanobacterial cell (Formighieri and Melis 2015). This was achieved upon expression of the *LaPHLS* gene under the strong endogenous *cpc* operon promoter and as a fusion protein with high abundance in cyanobacteria phycocyanin β-subunit (Formighieri and Melis 2016). The resulting *Synechocystis* transformants produced β-phellandrene as the major terpene product (88%), along with a small amount of β-myrcene, while no limonene was detected. This was a distinct and interesting feature of monoterpenes mixture obtained by heterologous expression of *LaPHLS* in cyanobacteria (Formighieri and Melis 2014b, 2015), and one that differed from the product profile obtained in vitro (Demissie et al. 2011).

β-Phellandrene is an important constituent of the essential oils in different plant species. The glandular trichomes found on the surface of leaves and stems of *Solanum lycopersicum* (tomato) were reported to contain β-phellandrene (1 mg g^{-1} leaf dry weight), followed by smaller amounts of limonene, α-phellandrene and δ-2-carene. A β-phellandrene synthase was shown to be highly expressed in tomato trichomes, and to specifically use neryl-diphosphate (NPP) as substrate instead of geranyl-diphosphate (GPP). A neryl-diphosphate synthase (NPPS) was also identified as the enzyme catalyzing the formation of NPP from the universal terpenoid precursors dimethylallyl-diphosphate (DMAPP) and isopentenyl-diphosphate (IPP) (Mahmoud and Croteau 2002; Schilmiller et al. 2009). When assayed in vitro with NPP, the profile of monoterpenes produced by SlPHLS was nearly identical with the profile of monoterpenes found in tomato trichomes (Schilmiller et al. 2009).

β-Phellandrene was additionally identified to be a constituent of the terpenoid oleoresin, which is used as a chemical and physical barrier against insect and pathogen attack by conifer trees. Oleoresin is stored in resin ducts of conifer bark, wood and needles (Hall et al. 2013). β-Phellandrene was found to accumulate up to 12 mg g^{-1} dry weight in leader stem and needles of three-year-old trees (Hall et al. 2013). β-Phellandrene synthases were identified by transcriptome analysis both in lodgepole pine (*Pinus contorta*) and jack pine (*Pinus banksiana*). In particular, two *P. contorta* and one *P. banksiana PHLS* sequences were identified, encoding proteins that have 95–99% identity. When assayed in vitro, these enzymes converted GPP into β-phellandrene, representing 82–88% of the overall terpene product (Hall et al. 2013).

Transcriptome mining was also used to isolate β-phellandrene synthase encoding sequences in *Picea sitchensis* (Sitka spruce). Four PHLS were identified that share 99% aminoacid identity, suggesting a recent gene duplication event. When assayed in vitro, these enzymes converted GPP into β-phellandrene as the major product (~ 60%), along with β-pinene (~ 20%) and α-pinene (~ 12%) (Keeling et al. 2011).

Screening of cDNA libraries also resulted in the isolation of a β-phellandrene synthase from *Abies grandis* (grand fir) that contributes to production of turpentine. In vitro, the enzyme yielded β-phellandrene as the major product (52%), along with β-pinene (34%), α-pinene (8.5%) and limonene (6%) (Bohlmann et al. 1999). Despite a similar monoterpenes profile, the PHLS from grand fir was only 70% identical to the PHLS proteins of Sitka spruce, suggesting that the gene function evolved independently (Keeling et al. 2011).

In the present work, we sought to examine how and to what extent β-phellandrene synthase (*PHLS*) genes from different plants would perform in cyanobacteria. The β-phellandrene synthase (PHLS) proteins from *S. lycopersicum*, *Pinus banksiana*, *P. sitchensis* and *A. grandis* were heterologously expressed and characterized in the cyanobacterium *Synechocystis*. We show differences in terms of expression, activity, and product specificity of the aforementioned enzymes in *Synechocystis* in vivo. Employment of different PHLS enzymes could be a strategy to obtain distinct monoterpene blends of commercial interest.

Materials and methods

Synechocystis strains, recombinant constructs, and culturing conditions

Synechocystis sp. PCC 6803 was used as the recipient strain and referred to as the wild type (wt) in this study. The PHLS sequences from *S. lycopersicum* (tomato; ACO56896.1), *Pinus banksiana* (pine; AFU73854.1), *P. sitchensis* (Sitka spruce; ADZ45506.1), and *A. grandis* (grand fir; AAF61453.1), and the NPPS sequence from *S. lycopersicum* (ACO56895.1), were codon-optimized for expression in *Synechocystis*, after removal of the putative chloroplast transit peptide, as predicted by ChloroP (Emanuelsson et al. 1999). The resulting nucleotide sequences (Supplementary Materials) were synthesized at Biomatik (http://www.biomatik.com/) with the NdeI and BglII restriction sites at the 5′ and 3′-end, respectively, for subsequent cloning in the corresponding sites of the CpcB•PHLS + Cpc plasmid. This plasmid was the same as that previously employed for expression of the *L. angustifolia* (lavender) PHLS in fusion with the *Synechocystis* phycocyanin β-subunit (CpcB) under control of the strong *cpc* operon promoter (Formighieri and Melis 2015). The NPPS encoding sequence, including the CpcA ribosome-binding site, was additionally cloned in an operon configuration downstream of the *SlPHLS* via BglII and NotI restriction sites. The recombinant plasmids used in this work have been deposited and can be made available through Addgene (<https://www.addgene.org/Anastasios_Melis>).

Synechocystis transformations and growth conditions followed established protocol (Williams 1988; Eaton-Rye 2011). Wild type and transformants were maintained on 1% agar BG11 media supplemented with 10 mM TES-NaOH (pH 8.2) and 0.3% sodium thiosulfate. Liquid cultures in BG11 were buffered with 25 mM phosphate (pH 7.5) and incubated under continuous low-stream bubbling with air at 28 °C. Transgenic DNA copy homoplasmy was achieved with cells incubated on agar in the presence of 30 µg/mL chloramphenicol, 5 mM glucose, under illumination of 170 µmol photons m^{-2} s^{-1}.

Genome integration of the recombinant cassette in the *cpc* locus, and attainment of transgenic DNA copy homoplasmy were verified by genomic DNA PCR analysis, using primers cpc_us and cpcA_Rv (Formighieri and Melis 2015). The cpc_us primer (5′- CCATTAGCAAGG CAAATCAAAGAC -3′) was also coupled in PCR reactions with specific oligonucleotide primers designed to recognize each PHLS sequence, as follows: 5′-AATCCA GGCACTGTGGGAAG-3′ (SlPHLS_Rv), 5′-CACGAC CGATGCCTTTCTC-3′ (PbPHLS_Rv), 5′-TTTCGAGCT TCTAATCGTGGC-3′ (PsPHLS_Rv), 5′-ATTGCGAGT TTCCAACCGAG-3′ (AgPHLS_Rv). Presence of the NPPS sequence was verified in a PCR reaction using the specific oligonucleotide (NPPS_Fw, 5′-TCGCTGGGC CAAAGATAAGG-3′) and cpcA_Rv (5′- GGTGGAAAC GGCTTCAGTTAAAG -3′).

Protein analysis and monoterpenes production by *Synechocystis* transformants

Protein extraction from cell lysates was performed as described (Formighieri and Melis 2015). Total cell proteins were resolved by SDS-PAGE and visualized by Coomassie stain.

Monoterpenes production and separation from the *Synechocystis* cultures was performed as described (Bentley et al. 2013; Formighieri and Melis 2014a, 2015). Briefly, cells from mid-growth cultures were pelleted and resuspended in fresh growth medium at $OD_{730\ nm} = 0.5$, briefly bubbled with 100% CO_2 to fill the headspace of the gaseous–aqueous two-phase reactor (Bentley and Melis 2012), sealed and incubated for 48 h in the light. Monoterpene hydrocarbons spontaneously diffused from the cell interior and accumulated as floating compounds on the surface of the liquid medium. They were collected from the surface of the transformant cultures upon addition of a known volume of hexane overlayer, applied at the end of the 48 h incubation period. Monoterpene products were analyzed by UV-absorbance spectrophotometry and sensitive gas chromatography (GC-FID) (Formighieri and Melis 2014b, 2015). For PsPHLS and AgPHLS, whose corresponding *Synechocystis* transformants yielded low levels of monoterpene products, a GC-FID splitless injection mode was used instead of a split ratio of 10.

Accession numbers of the genomic DNA/translation sequences employed in this work

GenBank accession numbers of the original cDNA and protein sequences used in this work. Readers are also directed to the Supplementary Materials section of this publication for a view of the *Synechocystis* codon-optimized version of these genes that were actually used in this work.

- *Solanum lycopersicum PHLS*: FJ797957.1/ACO56896.1,
- *Solanum lycopersicum NPPS1*: FJ797956.1/ACO56895.1,
- *Pinus banksiana PHLS*: JQ240302.1/AFU73854.1,
- *Picea sitchensis* PHLS: HQ426169.1/ADZ45506.1,
- *Abies grandis PHLS*: AF139205.1/AAF61453.1,
- *Escherichia coli cmR*: V00623.1/CAA23900.1,
- *Synechocystis* PCC 6808 *cpcB*: U34930.1/AGF50922.1.

Results

Solanum lycopersicum PHLS expression and activity in *Synechocystis* transformants

The DNA sequence encoding the *S. lycopersicum* PHLS (*SlPHLS*) was codon-optimized and expressed in *Synechocystis* as a fusion protein with the highly expressed in cyanobacteria phycocyanin β-subunit encoding *cpcB* gene under control of the strong endogenous *cpc* operon promoter. The chloramphenicol resistance (*cmR*) cassette was also inserted in this construct, downstream of the *SlPHLS,* followed by the other endogenous *cpc* operon genes (Fig. 1a). This strategy proved to be successful in over-expressing the PHLS from *L. angustifolia* (Formighieri and Melis 2015). High concentrations of the PHLS enzyme in the cell helped to overcome limitations in the rate and yield of monoterpene production due to the slow catalytic activity ($K_{cat} = \sim 3\ s^{-1}$) of terpene synthases (Formighieri and Melis 2015, 2016). A second

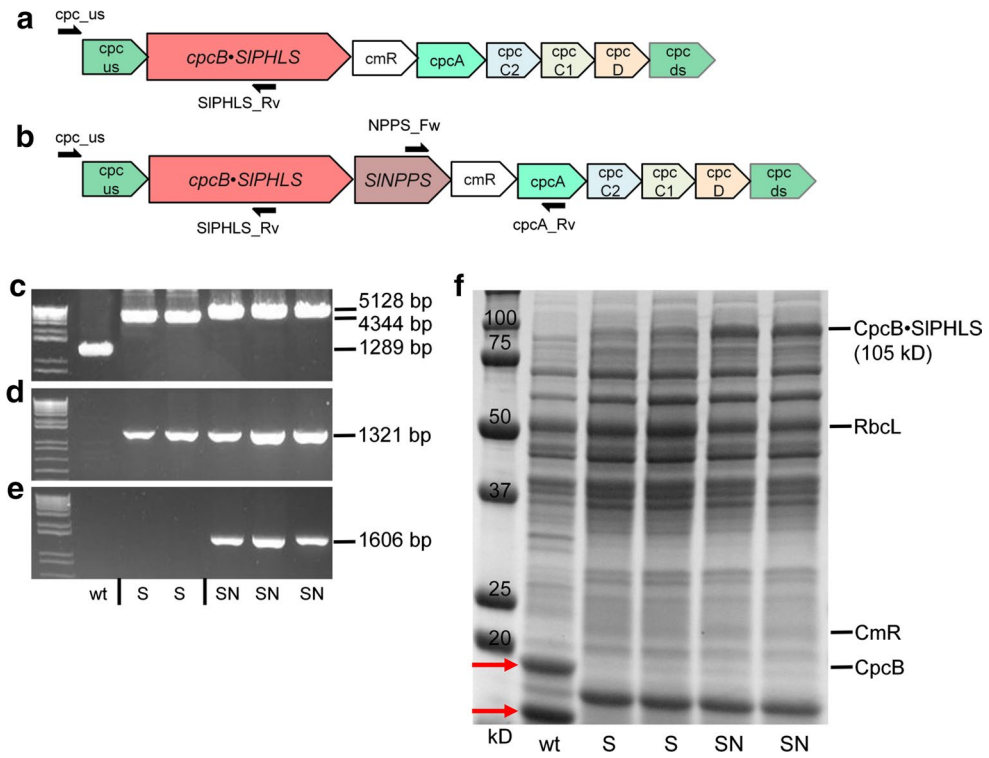

Fig. 1 Heterologous expression of *S. lycopersicum* (tomato) β-phellandrene synthase (SlPHLS) and neryl-diphosphate synthase (SlNPPS) in *Synechocystis*. **a** Recombinant construct for expression of SlPHLS as a fusion to the phycocyanin β-subunit (CpcB) in the *cpc* genomic locus. **b** Recombinant construct for co-expression of the CpcB•SlPHLS fusion construct with the NPPS. **c** Genomic PCR analysis of wild type and transformant *Synechocystis* with cpc_us and cpcA_Rv primers. **d** Genomic PCR analysis with cpc_us and SlPHLS_Rv primers. **e** Genomic PCR analysis with NPPS_Fw and cpcA_Rv primers. Location of the primers is shown as arrows in panels **a** and **b**. S denotes two independent CpcB•SlPHLS transformant lines, while SN denotes three independent CpcB•SlPHLS + NPPS transformant lines. **f** SDS-PAGE resolution and Coomassie stain of total cell protein extracts from *Synechocystis* wild type and transformants. The CpcB•SlPHLS fusion protein and the native CpcB are marked as 105 kD and 18 kD polypeptides, respectively. Molecular weight markers are shown on the left-most lane and expressed in kD

construct (Fig. 1b) was designed to co-express *SlPHLS* with the neryl-diphosphate synthase of *S. lycopersicum* (*SlNPPS*) in an operon configuration. *Synechocystis* is endowed with an endogenous pool of GPP, but it is not known if it also possesses NPPS activity. Transformation with the *SlNPPS* gene aimed to test for this possible hypothesis. The second construct tested the requirement of NPP as a substrate for the catalytic activity of SlPHLS.

Each construct was separately integrated in the *cpc* genomic locus of *Synechocystis* by double homologous recombination. The resulting transformants were screened by genomic DNA PCR analysis to test for the correct genomic locus integration of the recombinant genes and attainment of transgenic DNA copy homoplasmy. A PCR amplifying the *cpc* upstream-to-*cpcA* region resulted in a 5128 bp product with the CpcB•SlPHLS + NPPS transformants, a 4344 bp product with CpcB•SlPHLS, and a 1289 bp product with the wild type (Fig. 1c). PCR amplification of the *cpc* upstream-to-*SlPHLS* region gave a 1321 bp product in the transformants only, but not in the wt (Fig. 1d), while amplification of the *SlNPPS*-to-*cpcA* specifically showed presence of the NPPS encoding sequence in the CpcB•SlPHLS + NPPS transformants (Fig. 1e, 1606 bp product).

Protein expression analysis was then performed by SDS-PAGE of total cell extracts followed by Coomassie staining (Fig. 1f). While the CpcB 19 kD β-subunit and CpcA 15 kD α-subunit of phycocyanin (Fig. 1f, marked by red arrow) are the most abundant proteins in wild type *Synechocystis* extracts (Fig. 1f, wt), the native *cpcB* gene was replaced by the *cpcB•SlPHLS* fusion in the transformants. The resulting CpcB•SlPHLS fusion protein could be seen in the Coomassie stained gel with an expected molecular weight of 105 kD, both in CpcB•SlPHLS and CpcB•SlPHLS + NPPS transformants (Fig. 1f), offering clear evidence of protein over-expression. Traces of the CmR protein could also be seen in the ~ 23 kD region. In contrast, the NPPS protein could not be detected in the CpcB•SlPHLS + NPPS transformants upon Coomassie staining, indicating a lower level of expression.

In vivo activity of SlPHLS was assayed by measuring monoterpene hydrocarbons production by the CpcB•SlPHLS and CpcB•SlPHLS + NPPS *Synechocystis* transformants. The monoterpene products were collected as floater molecules from the surface of sealed cultures upon dilution with a known volume of hexane and upon siphoning off the top lipophilic phase. The hexane extracts from the CpcB•SlPHLS + NPPS transformants showed distinctive UV-absorbance spectra with a peak wavelength at 232 nm (Formighieri and Melis 2016), suggesting the presence of β-Phellandrene (Fig. 2a, CpcB•SlPHLS + NPPS). In contrast, the hexane extracts from the wild type and the CpcB•SlPHLS transformants resulted in a featureless flat absorbance (Fig. 2a, wt, CpcB•SlPHLS). This outcome was

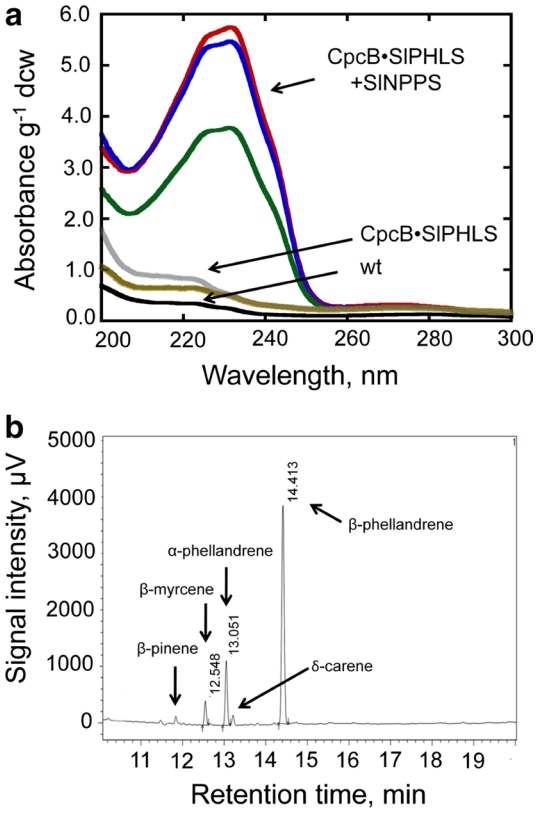

Fig. 2 Monoterpenes production by *Synechocystis* transformants expressing the SlPHLS construct with or without the NPPS transgene. Cells in liquid culture were grown photoautotrophically for 48 h. **a** UV-absorbance spectra of hexane extracts from *Synechocystis* CpcB•SlPHLS + NPPS and CpcB•SlPHLS transformants, normalized on per g of dry cell weight (dcw) and compared to wild type (wt) extracts. Red, blue, and green traces show the productivity of three independent CpcB•SlPHLS + NPPS transformants lines. **b** GC-FID analysis of the monoterpenes isolated from the CpcB•SlPHLS + NPPS transformants. β-Phellandrene, α-phellandrene and β-myrcene were detected as the main terpene products with retention time of 14.413, 13.051, and 12.548 min, respectively

expected for the wild type that is not endowed with the genes for monoterpene biosynthesis, but it also indicated lack of hydrocarbons productivity by the CpcB•SlPHLS transformants. The latter is consistent with the notion that SlPHLS alone cannot use the endogenous GPP pool in cyanobacteria, but it requires heterologous synthesis of NPP as the monoterpene-generating substrate.

The monoterpene hydrocarbons profile of the CpcB•SlPHLS + NPPS transformants was additionally analyzed by GC-FID, showing the presence of a blend of monoterpenes produced under these conditions (Fig. 2b). β-Phellandrene was detected as the major product (74%), followed by α-phellandrene (20%) and β-myrcene (5%). Smaller amounts (~ 1%) of β-pinene and δ-2-carene were also detected. Limonene was identified in tomato trichome

extracts and apparently produced by the SlPHLS enzyme in vitro (Schilmiller et al. 2009). However, it was not detected upon heterologous expression of the SlPHLS in *Synechocystis*. It is concluded that heterologous expression of the PHLS from tomato in *Synechocystis* resulted in the generation of a different blend of monoterpene hydrocarbons than those detected in the natural plant host or when the PHLS enzyme was tested under in vitro conditions.

Pinus banksiana PHLS expression and activity in *Synechocystis* transformants

The DNA sequence encoding the *P. banksiana PHLS* (*PbPHLS*) was codon-optimized and expressed in *Synechocystis* in the *cpc* genomic locus as a fusion with *cpcB* (Fig. 3a). Correct genomic locus integration and transgenic DNA copy homoplasmy were tested by genomic DNA PCR analysis. The *cpc* upstream-to-*cpcA* genomic region was PCR amplified and resulted in a 3834 bp product with the transformants, as compared to the 1289 bp product corresponding to the wild type sequence (Fig. 3b). The *cpc* upstream-to-*PbPHLS* region was specifically amplified in the transformants only, resulting in a 1495 bp PCR product (Fig. 3c).

Protein expression was then investigated by SDS-PAGE analysis of total cell protein extracts. The CpcB•PbPHLS fusion protein was highly expressed in the *Synechocystis* transformants, clearly visible upon Coomassie staining of the gel (Fig. 3d, CpcB•PbPHLS, expected molecular weight of 84 kD).

When assayed for monoterpene production, the CpcB•PbPHLS transformants showed a distinctive UV-absorbance spectrum of the hexane extracts as compared to the wild type, suggesting activity of the PbPHLS enzyme upon heterologous expression in *Synechocystis* (Fig. 4a). Analysis of the monoterpene products by GC-FID showed the presence of β-phellandrene as the dominant product (> 96%), suggesting high specificity of the PbPHLS enzyme toward the synthesis of β-phellandrene hydrocarbons in cyanobacteria (Fig. 4b). Considerably smaller amounts of β-pinene and β-myrcene were also detected (< 2%). The relatively higher specificity of cyanobacteria *PbPHLS* transformants for the β-phellandrene product affords an advantage over oleoresin extracts from *P. banksiana* that contain a mix of difficult to separate monoterpenes (Hall et al. 2013). It is also in contrast to the blend of monoterpene hydrocarbons obtained upon the in vivo expression of the *SlPHLS* gene in *Synechocystis* (Fig. 2b). As such, expression of the *PbPHLS* gene in cyanobacteria could be used for the generation of a purer monoterpene hydrocarbon product, when so desired.

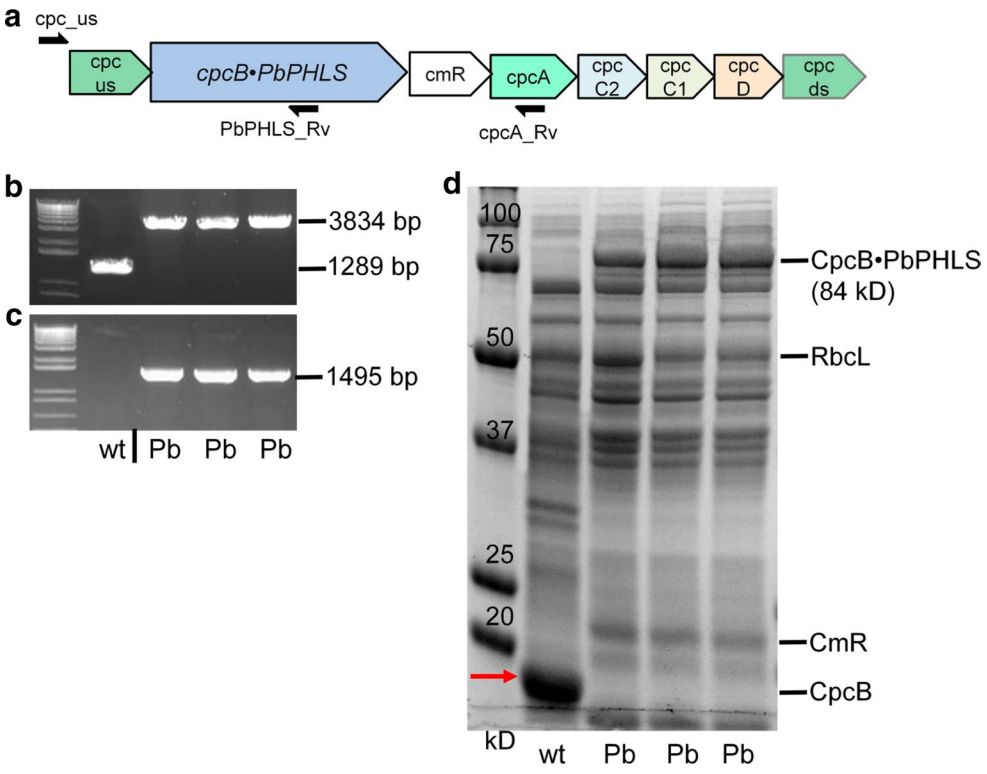

Fig. 3 Heterologous expression of *P. banksiana* (pine) β-phellandrene synthase (PbPHLS) in *Synechocystis*. **a** Recombinant construct for expression of PbPHLS as a fusion to CpcB in the *cpc* genomic locus. **b** Genomic PCR analysis with cpc_us and cpcA_Rv primers. **c** Genomic PCR analysis with cpc_us and PbPHLS_Rv primers. Location of the primers is shown as arrows in **a**. Pb denotes three independent transformants lines. **d** SDS-PAGE resolution and Coomassie stain of total cell protein extracts from *Synechocystis* wild type and transformants. The CpcB•PbPHLS fusion protein and the native CpcB are marked at 84 kD and 18 kD, respectively. Molecular weight markers are on the left side and expressed in kD

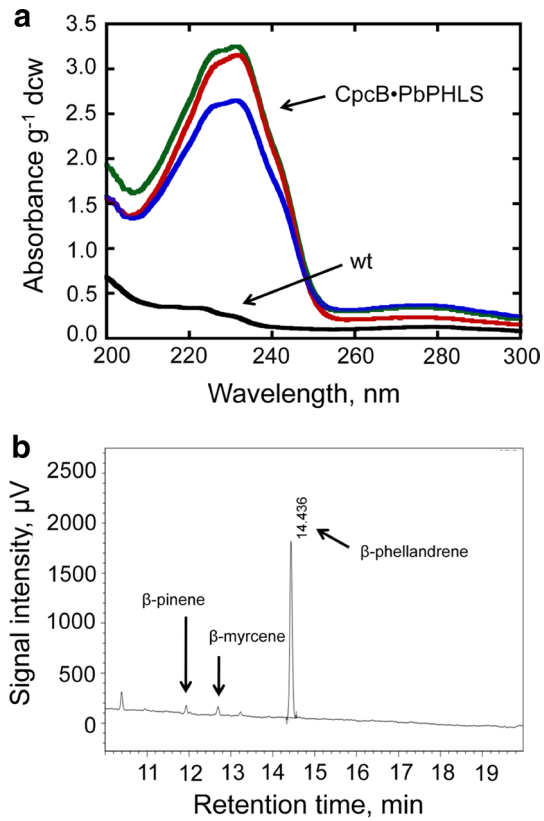

Fig. 4 Monoterpene production by *Synechocystis* transformants expressing PbPHLS. **a** UV-absorbance spectra of hexane extracts from *Synechocystis* CpcB•PbPHLS transformants, normalized on per g of dcw and compared to wild type (wt) extracts. **b** GC-FID analysis of the hexane extract from the CpcB•PbPHLS transformants, showing β-phellandrene to be the primary product with a retention time of 14.436 min

Picea sitchensis PHLS expression and activity in *Synechocystis* transformants

The DNA sequence encoding the *P. sitchensis* PHLS (*PsPHLS*) was codon-optimized and expressed as a fusion with *cpcB* in the *cpc* locus of the *Synechocystis* genome (Fig. 5a). Genomic DNA PCR analysis was then performed to genetically characterize the transformants. The *cpc* upstream-to-*cpcA* region was amplified by PCR and resulted in a 3837 bp product with the transformants. Absence of the 1289 bp product, corresponding to the wt sequence, showed attainment of transgenic DNA copy homoplasmy in the transformants (Fig. 5b). Genome integration of the *PsPHLS* encoding sequence was specifically verified by PCR amplification of the *cpc* upstream-to-*PsPHLS,* yielding a product of 1832 bp in the transformants only (Fig. 5c).

The CpcB•PsPHLS fusion protein, with an expected molecular weight of 84 kD, was detected upon Coomassie staining of electrophoretically resolved total protein cell extracts (Fig. 5d), indicating successful expression of the recombinant fusion protein. Heterologous expression of the *cpcB•PsPHLS* fusion resulted in relatively low yields of monoterpene production, as suggested by the low amplitude of UV-absorbance of exudates from the transformants (Fig. 6a), compared with production levels by the CpcB•SlPHLS (Fig. 2a) and CpcB•PsPHLS (Fig. 4a). GC-FID analysis (Fig. 6b) showed β-myrcene as the main monoterpene generated (62%), followed by smaller amounts of β-phellandrene (19%), α-phellandrene (14%), and β-pinene (5%). This profile was consistent with the UV-absorbance spectra of lipophilic extracts from these *Synechocystis* transformants. β-Phellandrene has an absorbance peak at 232 nm in hexane (Formighieri and Melis 2014a), while the absorbance max of hexane extracts from the CpcB•PsPHLS transformants shifted toward 224 nm, where the absorbance maximum of β-myrcene occurs (Fig. 6a). *PsPHLS* was additionally expressed under the *cpc* operon promoter in a non-fusion configuration with the *cpcB* gene, but this resulted in even lower yields of monoterpene production, likely related to lower protein expression levels (Formighieri and Melis 2014a), while the monoterpenes profile was the same as that shown in Fig. 6b (results not shown). Interestingly, the profile of monoterpene products obtained upon heterologous expression of *PsPHLS* in *Synechocystis* was different than that obtained from the recombinant enzyme in vitro (Keeling et al. 2011). These results also support the notion that heterologous expression in *Synechocystis* of the PHLS from *P. sitchensis* (Sitka spruce) results in the generation of substantially different profiles of monoterpenes than those obtained in the same cyanobacterial host with the lavender, tomato and pine PHLS enzymes, but also different from the monoterpenes profile of Sitka spruce extracts.

Abies grandis PHLS expression and activity in *Synechocystis* transformants

A corresponding DNA recombinant construct, as the ones employed for expression of the *PHLS* genes from the aforementioned plant species, was also made from the *A. grandis PHLS* (*AgPHLS*) for expression in *Synechocystis* (Fig. 7a). Genomic DNA PCR analysis confirmed the genetic locus and homoplasmy of the resulting *Synechocystis* transformants. PCR amplification of the *cpc* upstream-to-*cpcA* region resulted in a 3861 bp product with the transformants, and a 1289 bp product when using the wt genome as template (Fig. 7b). Genome integration of the *AgPHLS* encoding sequence was specifically tested upon amplification of the *cpc* upstream-to-*AgPHLS* region, resulting in an 1842 bp product in the transformants only (Fig. 7c). The CpcB•AgPHLS fusion protein was visually detected upon SDS-PAGE and Coomassie staining of total *Synechocystis*

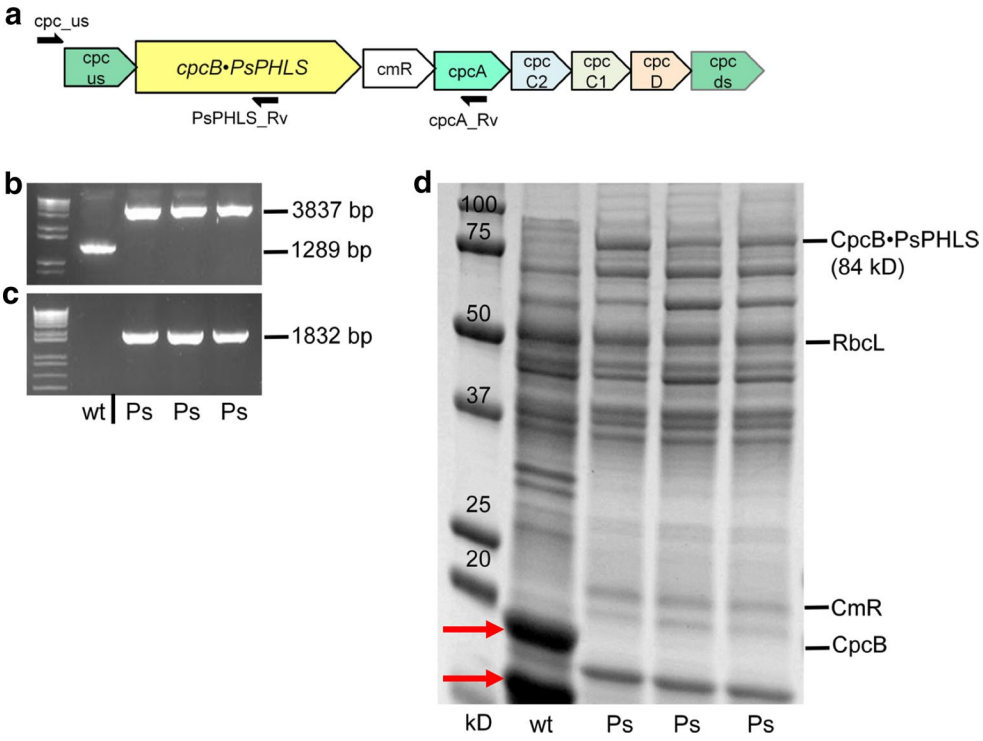

Fig. 5 Heterologous expression of *P. sitchensis* (Sitka spruce) β-phellandrene synthase (PsPHLS) in *Synechocystis*. **a** PsPHLS was expressed as a fusion to CpcB in the *cpc* genomic locus. **b** Genomic PCR analysis with cpc_us and cpcA_Rv primers. **c** Genomic PCR analysis with cpc_us and PsPHLS_Rv primers. Location of the primers is shown as arrows in (a). Ps denotes three independent transformants lines. **d** SDS-PAGE resolution and Coomassie stain of total cell protein extracts from *Synechocystis* wild type and transformants. The CpcB•PsPHLS fusion protein and the native CpcB are marked at 84 kD and 18 kD, respectively. Molecular weight markers are on the left side and expressed in kD

protein extracts, with an expected molecular weight of 86 kD (Fig. 7d).

When assayed upon heterologous expression in *Synechocystis*, the CpcB•AgPHLS construct yielded relatively low levels of monoterpenes, as shown by the low level of UV-absorbance (Fig. 8a), compared with production levels by the CpcB•SlPHLS (Fig. 2a) and CpcB•PsPHLS (Fig. 4a) constructs. Even lower yields were obtained upon expression of AgPHLS in a non-fusion configuration with the *cpcB* gene, corresponding to lower levels of protein expression (not shown). GC-FID analysis showed that the monoterpene exudates from the *CpcB•AgPHLS* transformant *Synechocystis* are composed of β-phellandrene (66%), β-myrcene (32%), and β-pinene (2%) (Fig. 8b). This GC–MS outcome is consistent with the features of the corresponding absorbance spectra (Fig. 8a) and reinforces the above results by showing that heterologous expression of the PHLS from *A. grandis* (grand fir) in *Synechocystis* results in the generation of a different blend of monoterpene hydrocarbons than those detected in the natural plant host or when the PHLS enzyme was tested under in vitro conditions.

Comparative analysis of PHLS function in *Synechocystis* transformants

Upon heterologous expression of the aforementioned PHLS proteins in *Synechocystis*, we observed differences in expression levels, activity and monoterpene products profile. Heterologous co-expression of SlPHLS and NPPS led on average to a total monoterpene yield of 0.6 mg g^{-1} dcw (Table 1), of which β-phellandrene accounted for 74%, followed by α-phellandrene (20%) and β-myrcene (5%, Table 2). Expression of SlPHLS, as a fusion to CpcB resulted in recombinant protein accumulation clearly visible in SDS-PAGE Coomassie stain. However, the NPPS protein was present at low levels in the transformants and could not be discerned in the Coomassie stain under these conditions (Fig. 1f). Because SlPHLS depends on the heterologous NPP synthase activity to supply the necessary NPP substrate, optimization of NPPS expression could further improve monoterpene yields.

Among the PHLS proteins from conifer trees, the PHLS from *P. banksiana* proved to be the most active in *Synechocystis* transformants, yielding an average of 0.33 mg β-phellandrene g^{-1} dcw (Table 1). PbPHLS also showed a higher specificity for β-phellandrene comprising the dominant product (Table 2). In contrast, heterologous expression of the PHLS from *P. sitchensis* and *A. grandis* resulted in lower product yields, although the recombinant proteins were expressed at sufficient levels and clearly visible in SDS-PAGE Coomassie stain of total cell protein extracts (Figs. 5, 7). These enzymes also produced a variable blend of monoterpenes (β-phellandrene, α-phellandrene, and β-myrcene, and β-pinene) with the acyclic monoterpene β-myrcene comprising higher relative amounts than those recorded with the other PHLS enzymes (Figs. 6, 8 and Table 2). β-myrcene synthesis by monoterpene synthase enzymes was associated to premature termination of the reaction (Srividya et al. 2015).

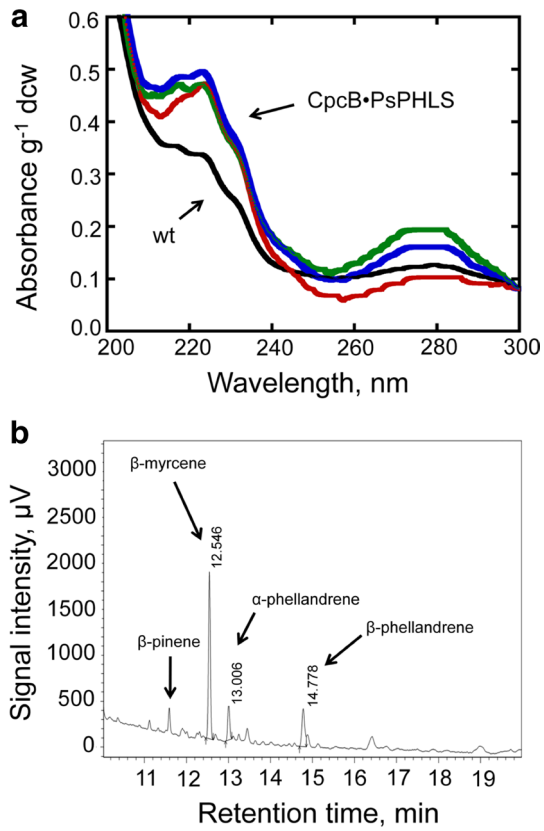

Fig. 6 Monoterpenes production by *Synechocystis* transformants expressing PsPHLS. **a** UV-absorbance spectra of hexane extracts from *Synechocystis* CpcB•PsPHLS transformants, as compared to the wild type. Spectra were normalized on per g of dcw. **b** GC-FID analysis of the hexane extract from CpcB•PsPHLS transformants. In this case, β-myrcene was the main product with a retention time of 12.546 min, followed by α-phellandrene and β-phellandrene at 13.006 min and 14.778 min of retention time, respectively

Discussion

The cyanobacterium *Synechocystis* was used as an alternative heterologous host for the production of plant essential oil compounds. As a case study, genes encoding the β-phellandrene synthase (*PHLS*) from divergent plant species (Schilmiller et al. 2009; Hall et al. 2013; Keeling et al. 2011; Bohlmann et al. 1999) were expressed in this cyanobacterium. β-Phellandrene (PHL) is a monocyclic monoterpene and is a good model product for the three types of monoterpenes, i.e., acyclic, monocyclic and bicyclic that are encountered in nature. Monoterpenes have several industrial applications in synthetic chemistry industry, perfumes, pharmaceuticals, pesticides, household cleaning supplies, and hydrocarbon biofuels. In this respect, the composition of the product is important as different monoterpenes in the essential oil mix will change the physical and organoleptic properties of the blend. However, our current knowledge about terpene synthases does not allow a confident prediction of the product blend, either from protein sequence analysis or structural modeling, thereby requiring experimental testing. This difficulty presents a limitation when designing heterologous systems for the production of essential oils for industrial application, since minor changes in the composition of the obtained mix can substantially alter the properties of the product. Our work aimed to evaluate heterologous expression of PHLS from different plant sources that could help future efforts favoring one enzyme over another to obtain specific essential oil blends.

The enzymes examined in the present work are all β-phellandrene synthases from divergent plant species, reported to catalyze the synthesis of β-phellandrene (Schilmiller et al. 2009; Hall et al. 2013; Keeling et al. 2011; Bohlmann et al. 1999). Despite this common catalytic activity, they substantially differ from one another in their amino acid sequence (Fig. S1). From the amino acid sequence alignment of different PHLS (Fig. S1), it is evident that there is a greater divergence in the N-terminal portion of the enzymes, as compared to the C-terminal region of these proteins. Overall, the higher degree of identity among the examined sequences is 70% between *P. sitchensis* and *A. grandis* PHLS, followed by 63% with the *P. banksiana* counterpart. These conifer enzymes are substantially different from the *L. angustifolia* PHLS showing only ~ 20% identity with the latter. The *S. lycopersicum* PHLS is also substantially different from the other PHLS enzymes examined in this work, having only ~ 15% identity with the rest. A rooted phylogenetic tree, based on the ClustalW amino acid sequence alignment (Fig. S1) is shown in Fig. 9. There is closer proximity, i.e., fewer nucleotide substitutions per site, among the conifer monoterpene synthases, and a higher degree of sequence divergence between the conifer monoterpene synthases and either the *L. angustifolia* PHLS or the *S. lycopersicum* PHLS, consistent with their taxonomic classification (Fig. 9).

Although the amino acid sequences are substantially different (Fig. S1), important conserved motifs among terpene synthases could be discerned as playing a role in the monoterpene hydrocarbons catalysis. In particular, the arginine-rich RR(×8)W signature motif is localized near the N-terminus (Fig. 10a, Catalytic site 1) and is part of an N-terminal strand that folds back onto the C-terminal domain, functioning to provide an overhang over the active site (Hyatt et al. 2007; Srividya et al. 2015). In the *S. lycopersicum* PHLS, this motif has an unusual alternative amino acid composition and probably structure shown as a KR(×9)W sequence (Fig. 10a).

The C-terminal α-domain contains the class-I (ionization-initiating) active site, characterized by the aspartate-rich DDxxD motif (Fig. 10b, Catalytic site 2) and the partially conserved (N/D)Dxx(S/T)xxxE sequence (Fig. 10c, Catalytic site 3) that coordinates the binding of three divalent

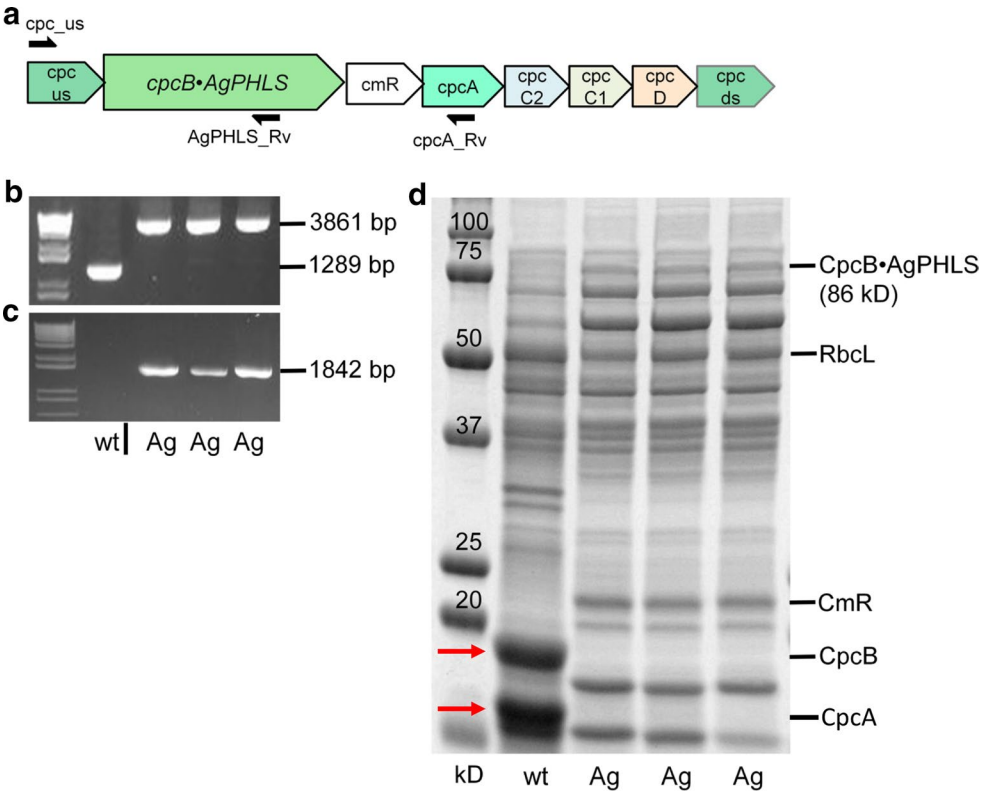

Fig. 7 Heterologous expression of *A. grandis* (grand fir) β-phellandrene synthase (AgPHLS) in *Synechocystis*. **a** AgPHLS was expressed as a fusion to CpcB in the *cpc* genomic locus. **b** Genomic PCR analysis with cpc_us and cpcA_Rv primers. **c** Genomic PCR analysis with cpc_us and AgPHLS_Rv primers. Location of the primers is shown as arrows in **a**. Ag denotes three independent transformants lines. **d** SDS-PAGE resolution and Coomassie stain of total cell protein extracts from *Synechocystis* wild type and transformants. The CpcB•AgPHLS fusion protein and the native CpcB are marked at 86 kD and 18 kD, respectively. Molecular weight markers are on the left side and expressed in kD

metal cations (Mg^{2+} or Mn^{2+}). The latter are required for substrate binding and activation (Demissie et al. 2011; Hyatt et al. 2007; Zhou et al. 2012).

Modeling the 3D structure of the PHLS proteins, performed with the RaptorX web server (Källberg et al. 2012), showed interesting features and differences in the folding of the respective polypeptides. The PHLS from *L. angustifolia* (Demissie et al. 2011; Bentley et al. 2013; Formighieri and Melis 2014a, 2015) was predicted to have a two-domain (αβ) structure and is similar to the class-I limonene synthase from *Mentha spicata* that served as the best template (2ongA, *p* value 2.43e-14) (Fig. 11a). The N-terminal strand (Fig. 11a, in red), that precedes the β-domain, is shown to fold back across the C-terminal α-domain to form a 'cap' that shields reactive carbocation intermediates from the aqueous medium (Hyatt et al. 2007; Srividya et al. 2015). Modeling of the CpcB•LaPHLS fusion protein showed the CpcB fusion moiety to be structurally separate from and folding to the southwest side of the LaPHLS configuration shown (Fig. 11b, blue structure, see also Chaves et al. 2017).

Terpene synthases are thought to derive from a common ancestor with a three (αβγ) domain structure (Fig. 11c; Trapp and Croteau 2001; 2001). During evolution, the γ-domain was lost from the monofunctional class-I terpene synthases, where catalytic sites 2 and 3 (Fig. 10) both are embedded in the α-domain of the C-terminal portion of the protein. In class-II terpene synthases, catalytic sites 2 and 3 are located between the N-terminal and γ and β domains of the enzyme, a feature that may have served to preserve the γ domain (Zhou et al. 2012). The N-terminal strand (Fig. 11a, in red), that precedes the β-domain, was also retained in the class-II enzymes, shown to fold back across the C-terminal α-domain to form a 'cap' that shields reactive carbocation intermediates from the solvent (Fig. 11c; Hyatt et al. 2007; Srividya et al. 2015). PHLS proteins from conifer trees (*Pinus banksiana*, *P. sitchensis* and *A. grandis*) were also modeled with a two-domain (αβ) structure (e.g. Figure 11a). However, based on their amino acid sequence, they showed higher similarity with sesquiterpene synthases from conifers, such as the bisabolene synthase from *A. grandis* (3saeA), rather than monoterpene synthases from angiosperm species (McAndrew et al. 2011).

Modeling of the 3D structure of the SlPHLS protein using the RaptorX web server (Källberg et al. 2012) showed a three-domain (αβγ) organization (Fig. 11c) with the best template being that of the diterpene abietadiene synthase from *A. grandis* (3s9vA, *p* value 9.58e-18). Modeling of the CpcB•SlPHLS fusion protein showed the CpcB domain to be folding toward the north side of the SlPHLS configuration (Fig. 11d, blue). Thus, it is of interest that whereas the *Lavandula angustifolia* PHLS has an αβ two-domain structure, the *S. lycopersicum* PHLS has the αβγ three-domain structure. Moreover, orientation of the leader CpcB fusion protein relative to the PHLS appears to be different in the

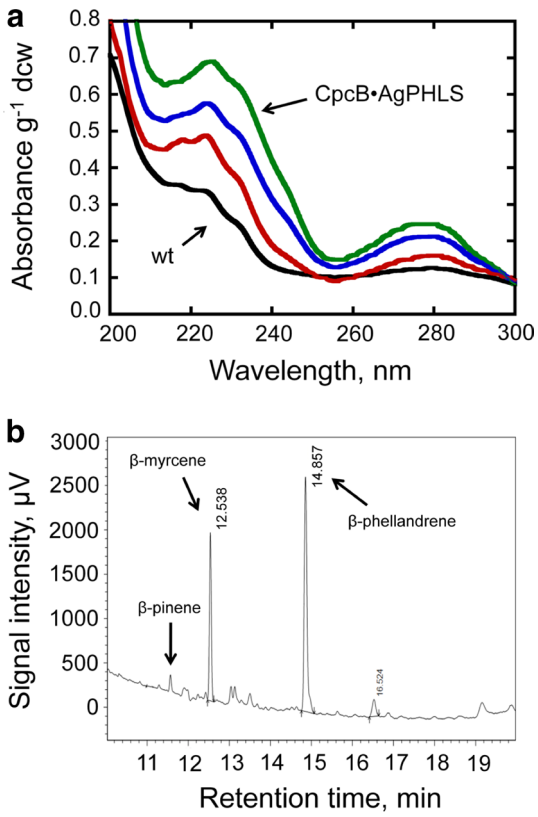

Fig. 8 Monoterpenes production by *Synechocystis* transformants expressing AgPHLS. **a** UV-absorbance spectra of hexane extracts from *Synechocystis* CpcB•AgPHLS transformants, normalized on per g of dcw and compared to wild type extracts. **b** GC-FID analysis of the hexane extract from CpcB•AgPHLS transformants that generated β-phellandrene and β-myrcene as the main monoterpenes. Retention times of the two monoterpenes products were 14.857, 12.538 min, respectively

Table 1 Photosynthetic carbon partitioning between monoterpenes and cellular biomass in *Synechocystis* transformants expressing the PHLS and NPPS from *S. lycopersicum*, or the PHLS from *Pinus banksiana*

	Monoterpene to biomass, mg g^{-1} dcw		
	Transformant lines tested		
	a	*b*	*c*
SlPHLS + NPPS	0.760 ± 0.10	0.597 ± 0.15	0.445 ± 0.06
PbPHLS	0.348 ± 0.08	0.330 ± 0.06	0.307 ± 0.02

Yields are expressed as mg of total monoterpenes relative to the increment in biomass observed during a 48 h culture incubation period. Three independent transformant lines were assayed for each genotype, with corresponding averages and standard deviations

Table 2 Monoterpene products profile obtained upon heterologous expression of β-phellandrene synthase in *Synechocystis* of the following enzymes: *L. angustifolia* (lavender) β-phellandrene synthase (LaPHLS), *S. lycopersicum* (tomato) β-phellandrene synthase and neryl-diphosphate synthase (SlPHLS + NPPS), *P. banksiana* β-phellandrene synthase (PbPHLS), *P. sitchensis* (Sitka spruce) β-phellandrene synthase (PsPHLS), *A. grandis* β-phellandrene synthase (AgPHLS)

	β-Phl (%)	α-Phl	β-Myr (%)	β-Pin	δ-Car
LaPHLS (Lavender)	88	n.d.	12	n.d	n.d
SlPHLS + NPPS (Tomato)	74	20%	5	< 1%	< 1%
PbPHLS (Pine)	> 96	n.d.	< 2	< 2%	n.d.
PsPHLS (Sitka spruce)	19	14%	62	5%	n.d.
AgPHLS (Grand fir)	66	n.d.	32	2%	n.d.

Monoterpenes are expressed as percentage of the total monoterpene blend photosynthetically generated

n.d. not detected

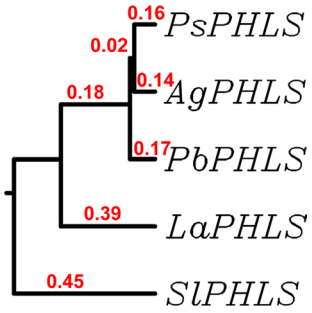

Fig. 9 Rooted phylogenetic tree (UPGMA) based on the ClustalW amino acid sequence alignment of the PHLS proteins heterologously expressed in *Synechocystis*. Branch lengths are proportional to the nucleotide substitutions per site

CpcB*LaPHLS (Fig. 11b) relative to the CpcB*SlPHLS construct (Fig. 11d). The different stereochemistry of the two fusion constructs may, at least in part, be responsible for the different catalytic activities and product specificities of the two enzymes.

Results from this work further suggest that the catalytic specificity of terpene synthases can also change depending on enzyme conformation and the cellular compartment and heterologous host in which they function. When the PHLS enzymes were expressed in the cytosol of the heterologous cyanobacterial host, they showed an ability to produce a variable blend of monoterpene hydrocarbons, in addition to β-phellandrene, whose composition and unique scent

Fig. 10 ClustalW amino acid sequence alignments of the conserved PHLS catalytic domains from different plant species. **a** (PHLS Catalytic site 1) The amino terminal side RR(x8)W signature motif. Note the unusual *S. lycopersicum* PHLS KR(x9)W motif in this region of the protein. **b** (PHLS Catalytic site 2) The mid protein α-domain containing the class-I (ionization-initiated) active site, characterized by the aspartate-rich DDxxD sequence. **c** (PHLS Catalytic site 3) The partially conserved (N/D)Dxx(S/T)xxxE sequence that coordinates binding of divalent metal cations (Mg^{2+} or Mn^{2+})

differed from what the same enzymes generate in their natural plant hosts, or when assayed in vitro. A primary reason for this discrepancy could be differences between the natural environment in which these enzymes function as opposed to the cyanobacterial environment employed in this study. The former is the chloroplast stroma in plants, whereas the latter is obligatorily the cytosol, as cyanobacteria are prokaryotes and do not possess organelles. The chemical environment and ionic strength of the cyanobacterial cytosol is likely different from that of the chloroplast stroma, and probably so from that employed under in vitro test conditions, thereby impacting the catalytic specificity of the enzymes. Interestingly, monoterpene synthases from angiosperms were reported to require either Mg^{2+} or Mn^{2+} in the ionization steps of the reaction to neutralize the negatively charged diphosphate group of the substrate (Schilmiller et al. 2009; Hyatt et al. 2007). In contrast, monoterpene synthases from conifers specifically require Mn^{2+}, while Mg^{2+} was an ineffective cation cofactor, and have the additional requirement for a monovalent cation (K^+) (Bohlmann et al. 1997; Green et al. 2009). Since changes in local concentrations of metal ions could affect activity and product specificity of the monoterpene synthases, modifications of *Synechocystis* growth media and culture conditions could be a complementary strategy to improve yields and composition toward desired monoterpene blends produced by cyanobacteria in vivo.

In conclusion, the present work describes the use of *Synechocystsis* (a cyanobacterium) as a heterologous host for the production of plant essential oils from sunlight, CO_2 and H_2O. β-Phellandrene synthase (*PHLS*) genes from different plants, when expressed in *Synechocystis*, enabled biosynthesis of variable monoterpene hydrocarbon blends, converting *Synechocystis* into a cell factory that photosynthesized and released useful products. Moreover, the variable

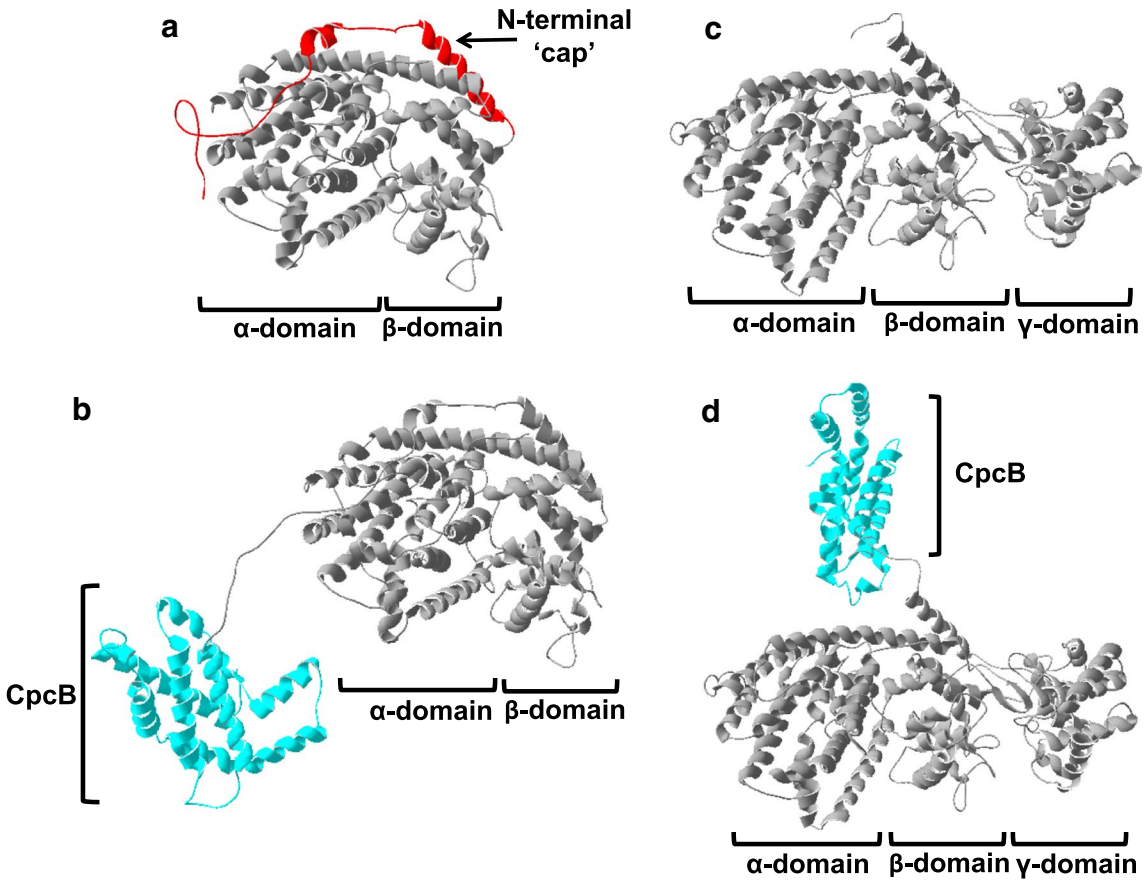

Fig. 11 Modeling of protein folding by the RaptorX web server (Källberg et al. 2012) of *L. angustifolia* PHLS and *S. lycopersicum* PHLS protein structures. **a** Predicted structure of the LaPHLS protein, showing the αβ domains and the N-terminal strand folding back across the C-terminal α-domain (in red). Best template: limonene synthase (2ongA), *p* value 2.43e-14. **b** CpcB•LaPHLS fusion protein structure, where the CpcB moiety is predicted to be structurally independent and not interfering with LaPHLS activity. **c** Predicted structure of the SlPHLS protein, showing the αβγ domains. Best template: abietadiene synthase (3s9vA), *p* value 9.58e-18. **d** CpcB•SlPHLS fusion protein structure, where the CpcB moiety is predicted to be structurally at right angles and, hence, not interfering with reactant access to SlPHLS

profile of monoterpene products emanating from the heterologous transformation differed from the products that are naturally found in plant extracts, and was also different from the products obtained upon in vitro assays of the recombinant proteins. This unexpected property is of interest, as it could be the source of terpene blends with distinct chemical properties and scents, i.e., of commercial value in applications by the cosmetics, pharmaceutical and potentially other industries.

Author contributions statement CF and AM designed the project and CF conducted the experimental work. CF and AM wrote the manuscript.

Compliance with ethical standards

Conflict of interest The authors declare that they have no conflict of interest.

Human participants and/or animals Research did not involve Human and/or Animal Subjects. Experimental protocols in this work were approved by the UC Berkeley Committee for Laboratory and Environmental BioSafety (CLEB).

Informed consent All authors have read and approved submission of this work.

References

Bentley FK, Melis A (2012) Diffusion-based process for carbon dioxide uptake and isoprene emission in gaseous/aqueous two-phase

photobioreactors by photosynthetic microorganisms. Biotechnol Bioeng 109:100–109

Bentley FK, García-Cerdán JG, Chen HC, Melis A (2013) Paradigm of monoterpene (β-phellandrene) hydrocarbons production via photosynthesis in cyanobacteria. BioEnergy Res 6:917–929

Bohlmann J, Steele CL, Croteau R (1997) Monoterpene synthases from grand fir (*Abies grandis*). cDNA isolation, characterization, and functional expression of myrcene synthase, (−)-(4S)-limonene synthase, and (−)-(1S,5S)-pinene synthase. J Biol Chem 272:21784–21792

Bohlmann J, Phillips M, Ramachandiran V, Katoh S, Croteau R (1999) cDNA cloning, characterization, and functional expression of four new monoterpene synthase members of the *Tpsd* gene family from grand fir (*Abies grandis*). Arch Biochem Biophys 368:232–243

Chaves JE, Rueda-Romero P, Kirst H, Melis A (2017) Engineering isoprene synthase expression and activity in cyanobacteria. ACS Synth Biol 6:2281–2292

Demissie ZA, Sarker LS, Mahmoud SS (2011) Cloning and functional characterization of β-phellandrene synthase from *Lavandula angustifolia*. Planta 233:685–696

Eaton-Rye JJ (2011) Construction of gene interruptions and gene deletions in the cyanobacterium *Synechocystis* sp. strain PCC 6803. Methods Mol Biol 684:295–312

Emanuelsson O, Nielsen H, von Heijne G (1999) ChloroP, a neural network-based method for predicting chloroplast transit peptides and their cleavage sites. Protein Sci 8:978–984

Formighieri C, Melis A (2014a) Regulation of β-phellandrene synthase gene expression, recombinant protein accumulation, and monoterpene hydrocarbons production in *Synechocystis* transformants. Planta 240:309–324

Formighieri C, Melis A (2014b) Carbon partitioning to the terpenoid biosynthetic pathway enables heterologous β-phellandrene production in *Escherichia coli* cultures. Arch Microbiol 196:853–861

Formighieri C, Melis A (2015) A phycocyanin-phellandrene synthase fusion enhances recombinant protein expression and β-phellandrene (monoterpene) hydrocarbons production in *Synechocystis* (cyanobacteria). Metab Eng 32:116–124

Formighieri C, Melis A (2016) Sustainable heterologous production of terpene hydrocarbons in cyanobacteria. Photosynth Res 130:123–135

Green S, Squire CJ, Nieuwenhuizen NJ, Baker EN, Laing W (2009) Defining the potassium binding region in an apple terpene synthase. J Biol Chem 284:8661–8669

Hall DE, Yuen MMS, Jancsik S, Quesada AL, Dullat HK, Li M, Henderson H, Arango-Velez A, Liao NY, Docking RT, Chan SK, Cooke JEK, Breuil C, Jones SJM, Keeling CI, Bohlmann J (2013) Transcriptome resources and functional characterization of monoterpene synthases for two host species of the mountain pine beetle, lodgepole pine (*Pinus contorta*) and jack pine (*Pinus banksiana*). BMC Plant Biol 13:80–94

Hyatt DC, Youn B, Zhao Y, Santhamma B, Coates RM, Croteau RB, Kang C (2007) Structure of limonene synthase, a simple model for terpenoid cyclase catalysis. Proc Natl Acad Sci USA 104:5360–5365

Källberg M, Wang H, Wang S, Peng J, Wang Z, Lu H, Xu J (2012) Template-based protein structure modeling using the RaptorX web server. Nat Protoc 7:1511–1522

Keeling CI, Weisshaar S, Ralph SG, Jancsik S, Hamberger B, Dullat HK, Bohlmann J (2011) Transcriptome mining, functional characterization, and phylogeny of a large terpene synthase gene family in spruce (*Picea* spp.). BMC Plant Biol 11:43–57

Lane A, Boecklemann A, Woronuk GN, Sarker L, Mahmoud SS (2010) A genomics resource for investigating regulation of essential oil production in *Lavandula angustifolia*. Planta 231:835–845

Mahmoud SS, Croteau RB (2002) Strategies for transgenic manipulation of monoterpene biosynthesis in plants. Trends Plant Sci 7:366–373

McAndrew RP, Peralta-Yahya PP, DeGiovanni A, Pereira JH, Hadi MZ, Keasling JD, Adams PD (2011) Structure of a three-domain sesquiterpene synthase: a prospective target for advanced biofuels production. Structure 19:1876–1884

Schilmiller AL, Schauvinhold I, Larson M, Xu R, Charbonneau AL, Schmidt A, Wilkerson C, Last RL, Pichersky E (2009) Monoterpenes in the glandular trichomes of tomato are synthesized from a neryl diphosphate precursor rather than geranyl diphosphate. Proc Natl Acad Sci USA 106:10865–10870

Srividya N, Davis EM, Croteau RB, Lange BM (2015) Functional analysis of (4S)-limonene synthase mutants reveals determinants of catalytic outcome in a model monoterpene synthase. Proc Natl Acad Sci USA 112:3332–3337

Trapp SC, Croteau RB (2001) Genomic organization of plant terpene synthases and molecular evolutionary implications. Genetics 158:811–832

Van Wagoner RM, Drummond AK, Wright JLC (2007) Biogenetic diversity of cyanobacterial metabolites. Adv Appl Microbiol 61:89–217

Williams JGK (1988) Construction of specific mutations in photosystem II photosynthetic reaction center by genetic engineering methods in *Synechocystis* 6803. Methods Enzymol 167:766–778

Zhou K, Gao Y, Hoy JA, Mann FM, Honzatko RB, Peters RJ (2012) Insights into diterpene cyclization from structure of bifunctional abietadiene synthase from *Abies grandis*. J Biol Chem 287:6840–6850